

BMAL1 and CLOCK control Polarization and Lumen Formation During Mammary Alveologenesis in 3D Culture

Jacob Larsen¹, Aridany Suarez-Trujillo², Kelsey Teeple¹, Jenna Schoonmaker¹, Karen Plaut¹ and Therasa Casey^{1#}

¹Purdue University

²Berry University

#Advisor

ABSTRACT

Circadian clock disruption decreased mammary development and impaired lactation in late gestation cows and mice. Transcriptional targets of the circadian clock genes BMAL1 and CLOCK include the cell-cell and cell-ECM proteins e-cadherin (CDH1) and zonula occludens-1 (ZO-1). The polarization and lumen formation of milk-producing acini is dependent on these junctional proteins. We hypothesized that if BMAL1 and CLOCK were disrupted, mammary epithelial cells (HC11) will have a reduced ability to form acini. Our objective was to measure the effect of BMAL1 gene deletion (BMAL1-KO) and CLOCK protein reduction (shCLOCK) in HC11 cells on the formation of acini and expression of CDH1 and ZO-1 in three-dimensional (3D) cultures. Cells were plated on Matrigel, embedded, and cultured to create 3D structures. ImageJ software was used to quantify the acini and found that the BMAL1-KO and shCLOCK lines formed fewer and smaller acini ($p < 0.05$). Confocal microscopy revealed that CDH1 was located along lateral membranes and ZO-1 was apically located in all three lines. Levels of CDH1 and ZO-1 were greater ($p < 0.05$) per unit volume of cell in the shCLOCK cell line. Live/dead staining of cells found little to no cell death across three lines. Transmission electron microscopy (TEM) of acini indicated less polarization of cells within BMAL1-KO and shCLOCK acini. Polarization of cells is required for formation of 3D structures and requires coordination of temporal-spatial cues. Disruption of circadian clocks results disturbs temporal organization of cellular processes and causes a reduced ability of cells to polarize and form acini.

Introduction

In mammals, the circadian timing system is essential for maintaining homeostasis in a changing environment. The system functions to coordinate internal physiology to regularly occurring external and internal signals, such as light/dark cycles.^{1,2} These temporal cues are received and integrated by the master clock in the suprachiasmatic nucleus (SCN) of the hypothalamus, which in turn sends out hormonal and nervous cues to peripheral clocks located in all organs of the body, including the mammary gland.¹ Timing information received by these peripheral clocks is integrated and used to establish circadian rhythms of gene expression. Five to ten percent of the genes expressed in a tissue exhibit circadian rhythms.³ The clock output genes are tissue specific and enable the coordination of circadian function with the activity of the organ.

The core molecular clock is a transcription-translation feedback loop of positive and negative elements.^{3,4} The positive arm is made up of the Brain and Muscle ARNT-Like 1 (BMAL1) gene and Circadian Locomotor Output Cycles Kaput (CLOCK) protein, which as a heterodimer function as a transcription factor that binds to an enhancer box (E-box) in the promoter region of target genes. Binding of BMAL1:CLOCK to the E-box drives the transcription of a multitude of genes including those that make up the negative arm of the transcription-translation feedback loop:

the Period (*PER1*, *PER2*, *PER3*) and Cryptochrome (*CRY1*, *CRY2*) genes. PER and CRY proteins function as suppressors and inhibit the binding of the BMAL1:CLOCK heterodimer to the E-box, and thus stop the further production of themselves. However, these proteins are broken down over time, so when their abundances decrease, the BMAL1:CLOCK heterodimer can bind again, and transcription resumes. The transcription-translation feedback loop has a 24-hour periodicity, resulting in circadian rhythms of gene expression that affect the timing of daily activity in cells.

Chromatin immunoprecipitation sequencing (ChIP-Seq) analysis of BMAL1 target genes in the mouse mammary epithelial cell line, HC11, found that among the potential BMAL1 targets were genes that regulate mammary morphogenesis.⁵ These include genes that regulate cell division, cell-cell adhesion molecules, and cell-extracellular matrix (ECM) adhesion molecules. Moreover, multiple BMAL1 target genes function to effect cell polarity including molecules that regulate ion and substrate transport across cells. Formation of milk-producing acini, which are spherical clusters of cells with a hollow lumen, requires epithelial cell proliferation, cell-cell and cell-ECM interactions, and a gain of polarity.^{6,7}

Previous studies of pregnant women found that sleep disruption, which disrupts circadian clocks, was related to a delay in the onset of lactation and lower rates of breast feeding during the first week after birth.^{3,8} In studies of dairy cattle, disrupting circadian clocks through exposure to chronic light-dark phase shifts during late pregnancy decreased the lumen to epithelial area ratio and mammary epithelial proliferation, which was associated with reduced milk production in the subsequent lactation.⁹ *Clock-Δ19* mice, which have a mutation in the CLOCK protein that causes a loss of circadian rhythmicity and decreased expression of clock controlled output genes, had poorer mammary development marked by a decreased lumen to epithelial area ratio in late pregnancy that was related to poorer lactation performance.¹⁰ Together, these findings support a role of the circadian timing system in the regulation of mammary development which is critical for lactation, but its specific mechanisms are not fully understood.

Our previous studies of mice revealed circadian rhythms of six core clock gene expression (*PER1*, *PER2*, *CRY1*, *CRY 2*, *BMAL1*, *CLOCK*) were attenuated in the mammary gland during the transition from pregnancy to lactation.¹¹ The abundance of BMAL1 and CLOCK proteins were increased significantly in mammary gland during the transition from pregnancy to lactation and were elevated across the 24 hour sampling period. Thus, continuously high levels of BMAL1:CLOCK may be important to lactation competence. The normal mouse mammary epithelial cell line, HC11, is frequently used for functional studies to understand the role of genes, pathways, and systems related to the regulation of growth, differentiation, and acini morphogenesis.¹²⁻¹⁴ To understand the role of BMAL1 and CLOCK in the regulation of mammary epithelial cell growth and differentiation, HC11 lines with BMAL1 knock out (BMAL1-KO)⁵ using CRISPR-Cas9 and CLOCK protein reduction using shRNA technology (shCLOCK)¹⁰ were established and deletion and knockdown were confirmed in previous experiments. The differing systems to knockout (remove) or knockdown of proteins enables the study and identification of non-circadian clock functions of the target gene, as well as reduced function of the core circadian clock in the cells. The rate of proliferation and growth across multiple days was increased in shCLOCK cells relative to the wild-type line.¹⁰ The shCLOCK line also had lower abundance of e-cadherin (CDH1) and P63 proteins, suggesting a potential for epithelial to mesenchyme transdifferentiation.^{15,16} Epithelial cells isolated from *Clock-Δ19* mouse mammary tissue had a diminished ability to form acini in culture.¹⁷ Growth curve analysis of BMAL1-KO cells found their doubling time was similar to wild-type cells, but cells died at a greater rate and cell death was related to accumulation of reactive oxygen species. We had identified multiple genes that encode proteins that regulate mammary epithelial cell differentiation and tissue morphogenesis as potential transcriptional targets in our ChIP-seq analysis of BMAL1 in HC11 cells.⁵

We hypothesized that the core circadian clock in the mammary gland plays a central role in formation of acini. Thus, if the BMAL1 gene is eliminated or levels of CLOCK, which heterodimerizes with BMAL1 to form the core clock transcription factor, are reduced, then the ability of mammary epithelial cells to form acini will also be reduced. A 3D cell culture system was used to quantify the effect of BMAL1 gene knockout (BMAL1-KO) and CLOCK protein reduction with shRNA (shCLOCK) on the number, size, and morphology of acini formed by each line. This was accomplished using light microscopy, confocal microscopy, and transmission electron microscopy to

gain an understanding how loss of function of these genes and the circadian clock system may inhibit mammary acini formation.

Materials & Methods

Cell Lines

Three lines were used for these experiments. The normal mouse mammary epithelial cell line, HC11,¹⁰ a monoclonal line of HC11 cells with the BMAL1 gene deleted using CRISPR-Cas9 knockout technology (BMAL1-KO),⁵ and a monoclonal line of HC11 cells with shRNA to knock down CLOCK protein levels (shCLOCK).¹⁰ The wild-type HC11 cell line was unedited and acted as the experimental control. Details of creation and validation of BMAL1-KO and shCLOCK lines have been described in previous experiments, but broad information is given briefly here.^{5,10} The BMAL1-KO line was created by knocking out the BMAL1 gene using ORIGENE's ARNTL Mouse Gene Knockout Kit (CRISPR, CAT#: KN301604, Rockville, MD, US).⁵ The manufacturer's protocol was followed to remove the target sequence, and knockout of the BMAL1 gene was confirmed with PCR and western blot analysis. PCR analysis demonstrated the donor cassette was integrated by positive amplification of guide RNA (gRNA) sequences. Western blot analysis found complete loss of the BMAL1 protein expression in the monoclonal line created using guide RNA1 (gRNA1), and Sanger sequencing confirmed genomic integration of a green fluorescent protein from the donor cassette. The shCLOCK line was created with shRNA targeted to *Clock* RNA in HC11 cells to knockdown the abundance of the CLOCK protein.¹⁰ This was accomplished by transfecting *Clock* shRNA plasmids into HC11 cells using the lipofection Attractene Transfection Reagent (Qiagen cat. no. 1051561) and selecting cells with hygromycin. Cells viable after 7 days of hygromycin selection were used to create clonal lines by dilutional cloning, and the effect of abundance of the *Clock* mRNA level was screened using qPCR. The monoclonal line transfected with sequence three (CGATGTCTCAAGCTGCAAATT) was used for these studies, as it was found to decrease levels of *Clock* mRNA by more than 70%, which was related to a significant reduction in CLOCK protein abundance.¹⁰

All cell lines were routinely cultured in RPMI growth media, which was composed of RPMI 1640 (50-020-PC, Mediatech Inc.) with 2 g/L sodium bicarbonate (S5761-500G, Sigma Life Science), 10% heat inactivated calf serum (26170-043, Gibco), 1% penicillin/streptomycin (15140-122, ThermoFisher Scientific), 10 ng/mL epidermal growth factor (E4127, Sigma-Aldrich), and 5 µg/mL insulin (IO516-5mL, Sigma-Aldrich).⁵ Cells were cultured in 5% CO₂ at 37°C. Cell were passaged when the cultures were at approximately 80% confluence at a 1:5 ratio, and the media was refreshed every 2 days. All studies were conducted in lines with less than 10 passages. Before 3D experimentation began, cell morphology was observed in 2-dimensional (2D) cultures in confluent undifferentiated and lactogen differentiated states. In this case, the cells were plated in a six well plate in RPMI growth media. On days 2 and 4 of culture, images were captured. On day 4, the media was changed to prehormone media, which contains the same components as the RPMI growth media, except no epidermal growth factor was included. After 48 hours in prehormone media, the cell media was changed to lactogenic media: RPMI supplemented with 10% calf serum, dexamethasone (0.1 µM), insulin (5 µg/mL), and prolactin (5 µg/mL; ovine prolactin: L6520-250IU, Sigma-Aldrich), and incubated for 96 hours, with media changed every 2 days. After 96 hours in lactogen media images were captured of cultures. Images of the cultures were captured with a Canon EOS Rebel T2i camera while using a Zeiss Axiovert 35 phase-contrast microscope on day 4 and day 8 to compare the undifferentiated and differentiated cells.

Drip Cultures

The approach to establish 3D drip cultures was developed and modified from several protocols.^{14,18-22} Each well of the 4-well chamber slide (1.8 cm²) was coated with 90 µL of cold growth factor reduced Matrigel (Corning Life Sciences). The 4-well chamber slide was placed in 5% CO₂ at 37°C in an incubator for 30 minutes to allow the Matrigel to

solidify. The cells were plated on top of the solidified Matrigel at a concentration of 13,000 cells/cm³ in a suspension of RPMI lactogenic growth media. The lactogenic growth media consisted of RPMI media supplemented with 5% serum, 1% penicillin/streptomycin, 5 µg/mL insulin, 5 µg/mL prolactin, and 0.375 ng/µL hydrocortisone (D8893-1mg, Sigma-Aldrich). After plating, cells were placed in 37°C incubator for 15 minutes to allow attachment to the Matrigel, and then the lactogenic growth media with 10% cold Matrigel was added drop by drop. This solution was made using a ratio of Matrigel to lactogenic growth media to Matrigel of 1:9, and afterwards, 200 µL was added to each well, so that the total volume in each well was 400 µL, and the final concentration of Matrigel was 5%. Following plating, cultures were placed into 37°C incubator, and lactogenic media without Matrigel was refreshed every 2 days until day 7.

Quantification of Acini and Morphological Features

On day 7 of culture, images of the acini were captured with an EOS Rebel T2i camera (Canon) while using an Axiovert 35 phase-contrast microscope (Zeiss) at 200x magnification. The wells were scanned from left to right, covering the entire well, and when an acinar structure was observed, an image was captured.

Acini, identified by their spherical-like shape and the presence of multiple cells within the structure, were counted and measured using ImageJ (National Institutes of Health). To measure the size of the acini the selection brush tool in ImageJ was used to outline acini, and then four measurements were taken: area, perimeter, minimum diameter, and maximum diameter. The circularity of each structure was determined using the following formula.²³

$$Circularity = \frac{4\pi * Area}{(Perimeter)^2}$$

Circularity determines how circular a shape is by using the relationship between area and perimeter; the circularity of a perfect circle is 1. After these measurements were collected, the acini were categorized within a cell line by size. Small acini were less than 150 µm², medium acini were between 150 µm² and 500 µm², and large acini were greater than 500 µm². Using Minitab, general linear model analysis followed by post-hoc Tukey's analysis were used to determine if cell line and experimental replicate affected the measured variables. Approximately 1,000 acini were counted in each of the three replicates of each of the cell lines to ensure representative sampling was achieved.

Immunofluorescence

For immunofluorescent staining and confocal microscopy, cells were plated for 3D cultures in 4-well chambered cover glass (1.8 cm², 155382PK, ThermoFisher). Culture medium was removed, and cells were washed two times with phosphate buffered saline (PBS). Cells were fixed in 4% formaldehyde at room temperature for 10 minutes; the formaldehyde was removed, and cells were washed three times with PBS for 5 minutes per wash. The cultures were then incubated for 15 minutes with 0.1% triton X-100 in PBS, followed by three washes with PBS for 5 minutes per wash. After the washes, non-specific binding was blocked by preincubating cells for 1 hour with 10% normal goat serum in PBST (PBS with 0.1 % Tween 20) with 50.6 mM glycine. After the blocking buffer was removed and the primary antibodies in solution were added, the cells were incubated in a humidified chamber overnight at 4°C. The primary antibodies were prepared in PBST-2% normal goat serum. The CDH1 primary antibody was a monoclonal rabbit antibody (1:100, Cell Signaling Technology, 24E10, #3195), and the ZO-1 primary antibody was a monoclonal rat antibody (1:100, Santa Cruz Biotechnology, R40.76, 33725). Samples were brought to room temperature for 30 minutes and washed three times with PBS for 10 minutes per wash. The cells were then incubated for 1 hour at room temperature with the secondary antibodies in PBST-2% normal goat serum. The anti-rabbit secondary antibody was an anti-rabbit IgG (H+L) produced in goats and conjugated with Alexa Fluor 555 (#4413). The fluorescence of this antibody was shown in green in our fluorescence images. The anti-rat secondary antibody was an anti-rat IgG (H+L)

produced in goats and conjugated with Alexa Fluor 647 (#4418). The fluorescence of this antibody is typically green; however, since a green stain was already being used, the color was changed to reddish-purple during data analysis for this experiment. Cultures were then washed six times with PBS for 10 minutes per wash and incubated for 10 minutes at room temperature with DAPI (1:1000 in PBS) for nuclear counterstaining. Cells were washed with PBS for 5 minutes and stored in PBS until confocal microscopy was conducted.

A Nikon A1R MP+ (Nikon Corporation) multiphoton confocal microscope was used at Bindley Bioscience Center at Purdue University to capture images of acini. The Z-stack images collected were analyzed using a protocol developed by Nikon for NIS Elements to determine the following parameters for each acinar structure: number of nuclei, total volume of CDH1 (μm^3), and total volume of ZO-1 (μm^3). Relative amounts of the cell-cell adhesion proteins were determined by dividing the total volume of each protein in a particular acinus by the number of nuclei counted previously in that same acinus. These values were then averaged across all the acini for a particular cell line for statistical analysis.

Minitab was used for statistical analysis, and a one-way ANOVA coupled with Tukey post-hoc test analysis was used to determine if there were significant differences in number of nuclei or adhesion proteins between the cell lines and experimental replicates. At least 140 acini were counted in both replicates of each of the cell lines to ensure representative samples were analyzed.

Live/Dead Staining

This experiment was conducted to determine if cell death played a role in the ability of the BMAL1-KO and shCLOCK cells to form 3D acini. To compare the amounts of live and dead cells within the 3D structures, the Live/Dead™ Viability/Cytotoxicity Kit for mammalian cells (Catalog # L3224, ThermoFisher Scientific) was used following manufacturer's protocol. Briefly, the live/dead assay reagents were warmed to room temperature. The 2 μM Calcein AM was diluted 1:2000, and the 4 μM of EthD-1 solution was diluted 1:500. To stain the cells, the media was aspirated from the cultures, which were washed twice with 1X PBS to remove all potential traces of serum. Then, 500 μL of staining solution was added directly on top of the Matrigel and was incubated at room temperature for 30 minutes. Images were collected using a Nikon A1R MP+ (Nikon Corporation) multiphoton confocal microscope at Bindley Bioscience Center at Purdue University.

Transmission Electron Microscopy

To visualize polarization of the cells within the acinar structures, transmission electron microscopy (TEM) was used. Cells were cultured for 7 days in the 4-well chamber slides with Matrigel as described above. On day 7, the cells were fixed in 2.5% glutaraldehyde in 0.1 M sodium cacodylate buffer, post-fixed in 1% osmium tetroxide containing 0.8% potassium ferricyanide, and en bloc stained in 1% uranyl acetate. Then, the structures were dehydrated with a graded series of ethanol, transferred into acetonitrile, and embedded in Embed 812 resin (Electron Microscopy Sciences). Thin sections were cut on a Leica EM UC6ultramicrotome and stained with 4% uranyl acetate and lead citrate. Images of the samples were acquired with a Gatan Orius camera on a FEI Tecani T12 electron microscope equipped with a tungsten source and operating at 80 kV in Purdue University's Electron Microscopy Core Facility.

Results

Characterization of Cell Lines

Our previous studies confirmed complete loss of BMAL1 protein in western blots of BMAL1-KO line⁵ and knock-down of CLOCK protein in the shCLOCK line.¹⁰ The dynamics of other expression of other core clock genes were disrupted by the genetic changes, demonstrating not only loss or reduction of BMAL1 and CLOCK in the respective lines, but disruption in the core circadian clock molecular system. Images captured of the 2D cultures show the distinct morphology of wild-type HC11, BMAL1-KO and shCLOCK lines after 4 days of growth, followed by 4 days of exposure to lactogenic media (Figure 1). HC11 cells exhibit a cobblestone morphology typical of normal mammary epithelial cells after 4 days in growth media (Figures 1A) and formed domes typical of mammary epithelial differentiation in 2D culture (Figure 1B). BMAL1-KO cells on day 4 of growth had numerous cytoplasmic vacuoles (Figure 1D) with minimal evidence of domes in lactogen differentiated 2D cultures (Figure 1E).²⁴ The shCLOCK cells had a more spindle-like appearance after 4 days in growth media (Figure 1G) with minimal evidence for dome formation in culture as well (Figure 1H).

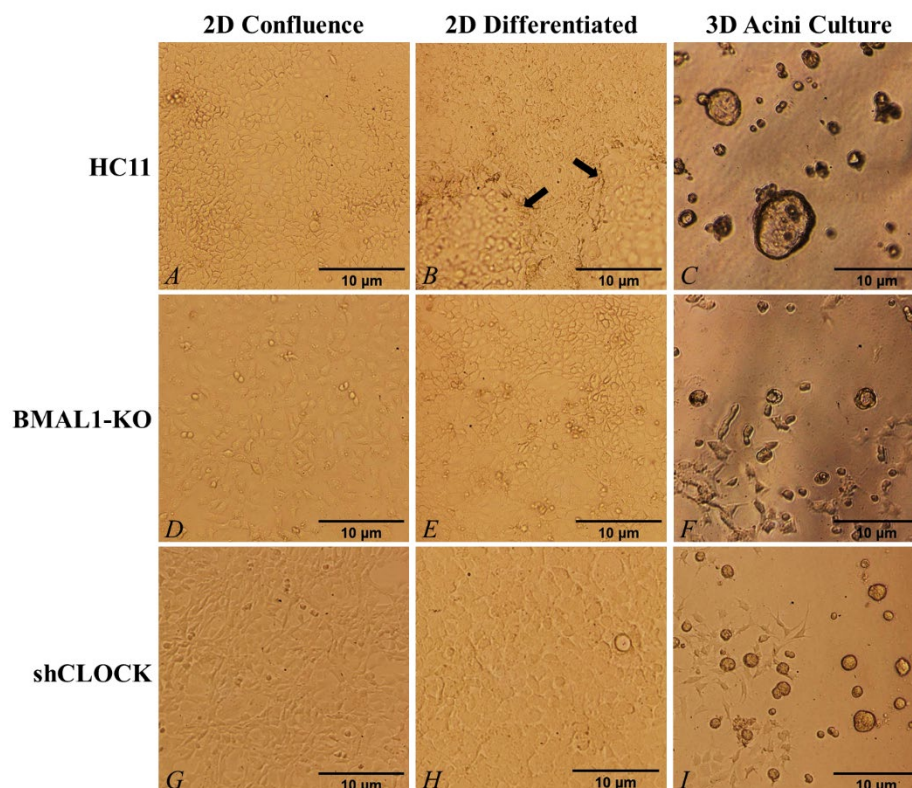


Figure 1. Qualitative analysis of acinar formation after various days in 2D and 3D cultures of images captured using phase-contrast microscopy at 100x magnification. Images show representative morphologies of HC11 (A – C), BMAL1-KO (D – F), and shCLOCK (G – I) cells and acini. Arrows in 1B indicate domes of typical mammary epithelial cell differentiation in 2D culture.

Images captured under phase-contrast microscopy across the 7 days in 3D culture demonstrate the progressive formation of acini by wild-type HC11 cells (Supplemental Figure S1). On day 2 of culture, simple clusters of cells formed, with no apparent lumen (Supplemental Figure S1A). As the structures grew, lumens began to form (Supplemental Figure S1B). By day 7, the size of acini had significantly increased, and lumen became apparent under phase-contrast microscopy (Supplemental Figure S1C).

The images on day 7 of 3D cultures using phase-contrast microscopy showed that size and morphology varied distinctly across the three cell lines. The HC11 acini were diverse in terms of their size and appeared to have large luminal area (Figure 1C). The BMAL1-KO acini were smaller than the HC11 acini and had very minimal evidence of the formation of lumens (Figure 1F). The BMAL1-KO cultures also had high levels of cells growing in 2D, which is indicative of a reduced ability to form acini, and the shCLOCK acini were small with no apparent lumen formation (Figure 1I).

Phase-contrast images were used to quantify differences in acini between the three cell lines (Table 1). The total number of acini formed per well of HC11 cells was approximately double ($p < 0.05$) the number of acini formed in cultures of BMAL1-KO and shCLOCK lines. The HC11 acini were larger in terms of area, perimeter, and minimum and maximum diameters when compared to the BMAL1-KO and shCLOCK lines. The BMAL1-KO and shCLOCK formed acini similar in size. There were no acini classified as large ($>500 \mu\text{m}^2$) in the BMAL1-KO and shCLOCK cultures, which were mostly represented by small acini. Analysis of circularity found that shCLOCK acini were the most circular out of the three cell lines.

Table 1. Size quantification of acini from phase-contrast microscopy images

| | HC11 | BMAL1-KO | shCLOCK |
|--|----------------------------------|--------------------------------|--------------------------------|
| Average No. of Acini per Well | 170 \pm 41.62 ^a | 80 \pm 17.44 ^b | 98 \pm 10.15 ^c |
| Size Distribution of Acini ¹ | | | |
| % Small | 42.25 ^a | 95.42 ^b | 95.58 ^b |
| % Medium | 37.79 ^a | 4.58 ^b | 4.42 ^b |
| % Large | 19.96 ^a | 0.00 ^b | 0.00 ^b |
| Average Area (μm^2) | 344.99 \pm 452.87 ^a | 82.65 \pm 39.65 ^b | 70.71 \pm 39.80 ^b |
| Average Perimeter (μm) | 62.80 \pm 35.64 ^a | 34.16 \pm 8.18 ^b | 30.80 \pm 8.28 ^b |
| Average Minimum Diameter (μm) | 17.04 \pm 9.41 ^a | 9.18 \pm 2.14 ^b | 8.59 \pm 2.11 ^b |
| Average Maximum Diameter (μm) | 20.63 \pm 11.42 ^a | 11.44 \pm 2.87 ^b | 10.13 \pm 2.86 ^b |
| Average Circularity (%) | 84.96 \pm 5.42 ^a | 85.49 \pm 5.56 ^a | 88.71 \pm 3.82 ^b |

Different letters indicate a significant difference between the lines at $p < 0.05$; ¹Size Distribution of acini: small $<150 \mu\text{m}^2$; medium $> 150 \mu\text{m}^2$ but $< 500 \mu\text{m}^2$; large $> 500 \mu\text{m}^2$.

IF Intensity Comparison & Quantification

Images captured of IF stained HC11 acini showed DAPI stained nuclei (Figure 2A), and CDH1 proteins located between adjacent cells (Figure 2B), which is consistent with adherens junction location. The ZO-1 protein staining was located apically, which is consistent with tight junction location (Figure 2C). Fewer DAPI stained nuclei were associated with acini in the BMAL1-KO and shCLOCK cultures (Figures 2D & 2G). CDH1 and ZO-1 stainings were also laterally and apically located, respectively, in BMAL1-KO (Figures 2E – 2F) and shCLOCK (Figures 2H – 2I) lines.

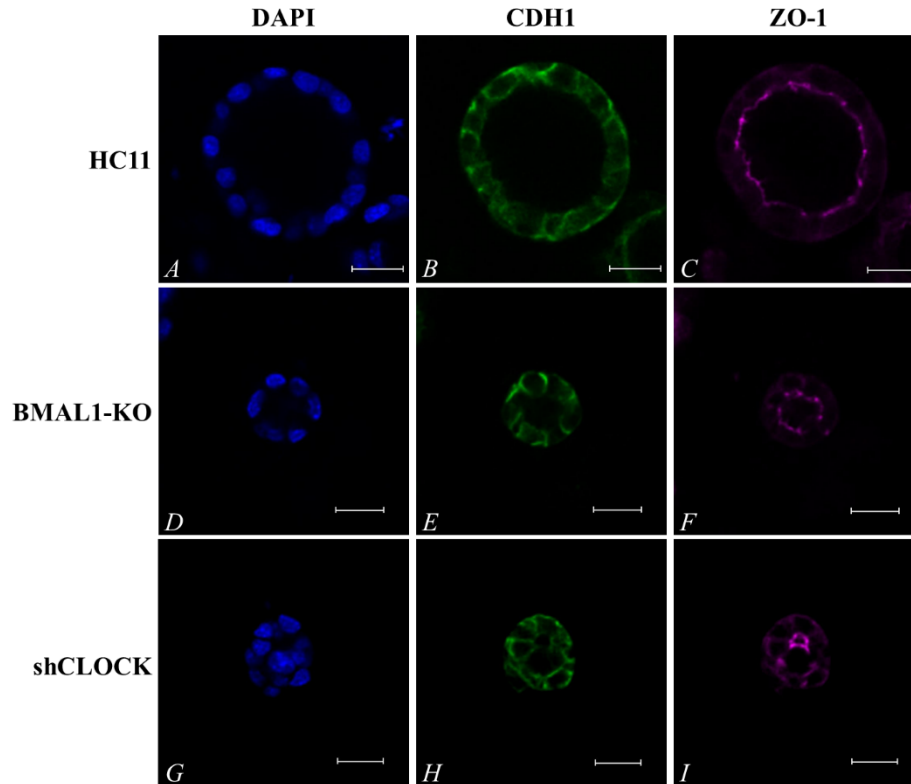


Figure 2. Comparison of the three cell lines after IF staining. The same three stains were used as shown previously to show the locations of nuclei (blue), CDH1 (green), and ZO-1 (purple) in the HC11 (A – C), BMAL1-KO (D – F), and shCLOCK (G – I) cell lines. Scale bars are equal to 20 μm .

The number of nuclei per acini and relative abundance of the adherens junction protein (CDH1) and the tight junction protein (ZO-1) stainings were quantified in confocal images (Table 2). The number of nuclei per HC11 acini was significantly greater ($p < 0.05$) than in BMAL1-KO and shCLOCK lines. There was no difference in the number of nuclei between the BMAL1-KO and shCLOCK lines. The relative abundance of CDH1 was greatest in shCLOCK acini; however, there was no difference between the HC11 and BMAL1-KO acini. The relative abundance of ZO-1 was greatest in shCLOCK, followed by BMAL1-KO, and then HC11 acini.

Table 2. Quantification of the number of nuclei and abundance of CDH1 and ZO-1 per acini volume in confocal images.

| | HC11 | BMAL1-KO | shCLOCK |
|--|----------------------------------|----------------------------------|----------------------------------|
| Average No. of Nuclei per Acini | 118.13 \pm 130.46 ^a | 33.78 \pm 44.38 ^b | 15.56 \pm 9.84 ^b |
| Relative Abundance of CDH1 (μm^3) | 145.70 \pm 125.00 ^a | 149.22 \pm 102.44 ^a | 450.43 \pm 217.98 ^b |
| Relative Abundance of ZO-1 (μm^3) | 71.16 \pm 82.15 ^a | 150.58 \pm 117.23 ^b | 215.29 \pm 150.32 ^c |

Different letters indicate a significant difference between the lines at $p < 0.05$.

Live/Dead Staining

To determine if the limitation of acini size was due to cell death in the shCLOCK and BMAL1-KO cultures, cells were live/dead stained and visualized using fluorescent microscopy. Overall, dead cells were scarce in the 3D cultures for all three cell lines and very few were associated with the acinar structures (Figure 3). On day 7, dead cells were

present in the HC11 and BMAL1-KO cultures as independent cells, but few were associated with the acinar structures (Figures 3A – 3B). The shCLOCK cultures appeared to have very few dead cells present in the cultures at all (Figure 3C).

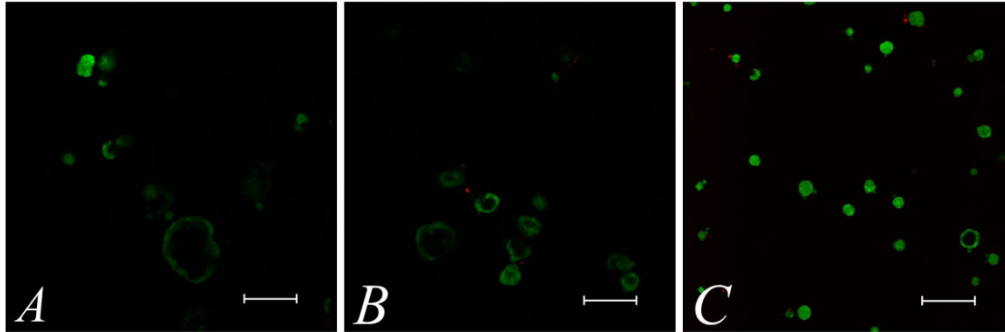


Figure 3. Qualitative analysis of live/dead staining of HC11 (A), BMAL1-KO (B), and shCLOCK (C) shows that cell death does not have an impact on the ability of the cells to form acini, since the dead cells (red) are not associated with the live cells (green) of the acini. Scale bars are equal to 100 μm .

Transmission Electron Microscopy

TEM was used to examine the microstructure of the cells of the acini, and it demonstrated differences in the overall size and confirmed differences in ability to form lumens between the HC11 (Figures 4A – 4C), BMAL1-KO (Figures 4D – 4F), and shCLOCK (Figures 4G – 4I) cell lines. Clear acini with lumens were observed in the HC11 and BMAL1-KO cell lines, although the BMAL1-KO line appeared to have smaller lumens overall. In addition, differences in polarity were observed; analysis of the images showed HC11 nuclei mostly located on the basal membrane, indicating polarization of the cells, whereas BMAL1-KO and shCLOCK cells exhibited less nuclear polarization within cells. Convolution of lateral membranes typical of differentiated mammary epithelial cells was evident in all three cell lines.²⁵ Microplicae were observed on the apical membrane of the HC11 cells, and on the apical and basal membranes of the BMAL1-KO and shCLOCK cells. Cell-cell junctional complexes were observed in HC11 and BMAL1-KO acini; however, shCLOCK acini had decreased evidence of these structures.

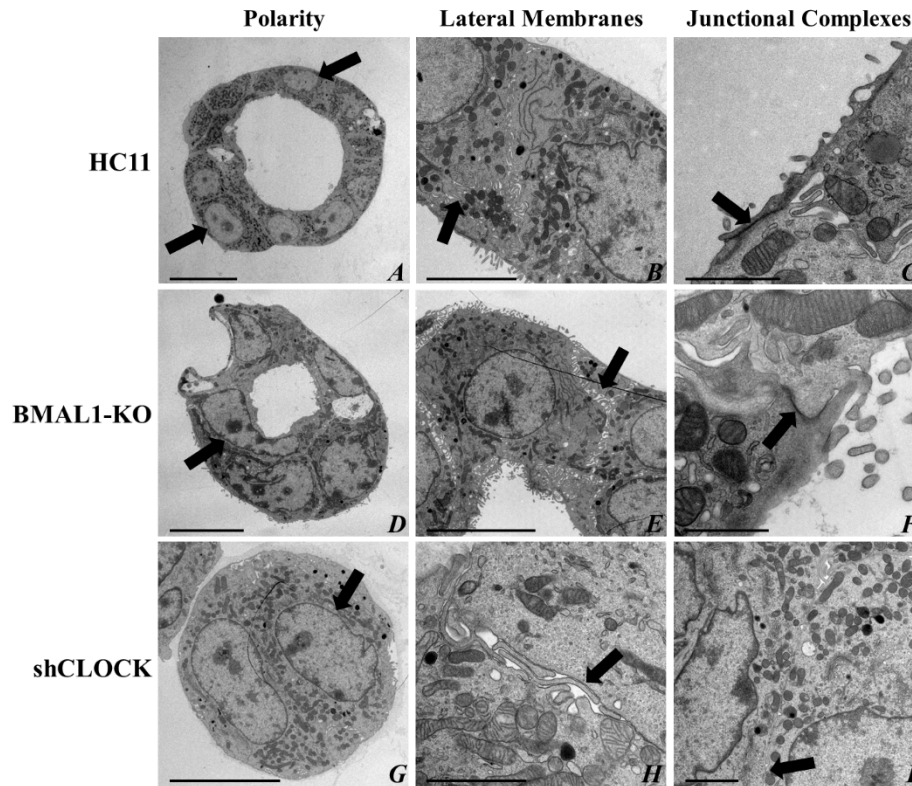


Figure 4. Qualitative analysis of transmission electron microscopy in HC11 (A – C), BMAL1-KO (D – F), and shCLOCK (G – I) cell lines. Images show differences in cell polarization (Column 1), convolution of lateral membranes (Column 2), and junctional complexes (Column 3) within acini of each cell line. Arrows in each image indicate the relevant aspects of the acinar structure. Scale bars vary throughout the figure but are equal to the following: A – 20 μm ; D, E, & G – 10 μm ; B – 5 μm ; C & H – 2 μm ; F & I – 1 μm .

Discussion

The knockout of BMAL1 and knockdown of CLOCK negatively impacted the ability of HC11 cells to form acini in three-dimensional cultures. This finding supports the hypothesis that the core circadian clock in mammary epithelial cells functions to regulate morphogenesis in the gland. In addition, it provides insight into our previous studies that found circadian disruption during pregnancy was associated with decreased mammary development and lower milk production. The decreased mammary development in dairy cattle and in mice with the *Clock- $\Delta 19$* mutation was characterized by a lower lumen to epithelial area ratio. Knockout of BMAL1 and reduced levels of CLOCK decreased the size and lumen of acini formed in culture. Therefore, decreased levels or function of these genes and proteins in mammary epithelial cells due to the genetic and environmental perturbations, respectively, may explain poorer mammary development.

Cells organize their functions both physically and temporally.²⁶ Temporal and physical organization form iterative loops during progressive differentiation and circadian clocks central to these loops. Clocks affect cell fate by controlling gene expression and protein synthesis and modification, influencing the timing of cell cycle and cellular differentiation from progenitor stem cells. Disruption of circadian clocks and component genes can thus affect these loops and processes and impair the ability to initiate coordinated cellular changes that need to proceed processes of synchronized tissue morphogenesis. The impact of circadian clock disruption varies with developmental time point. Circadian oscillations are silenced in embryonic stem cells and as cell differentiate circadian oscillation of gene

expression becomes more pronounced.²⁶ Our findings add to the growing body of literature that show the targeted alteration of core circadian clock in mammary epithelial cells results in differing phenotypes and are influenced by environmental factors, exemplified in part by differences in phenotype in 2D and 3D culture systems.

Due to their importance to fitness and survival, core clock genes underwent multiplicity events in vertebrates,²⁷ and molecular redundancy exists for all core clock genes with three *PER* two *CRY*, and paralogues of *BMAL1* and *CLOCK* being *BMAL2* and *NPAS2*, respectively. Although there is a fair amount of functional overlap of paralogues and homologues, the redundancy resulted in functional divergence, tissue specificity, and regulation of developmental processes.²⁸ For example, mice with homozygous deletion of *PER2* have diminished mammary ductal development during puberty but are able to develop normal lobuloalveolar structures and support pup growth during lactation.²⁹ Decreasing *PER2* abundance in a normal human mammary cell line with shRNA resulted in formation of large spherical clusters of cells in 3D culture that lacked lumens. Similarly, human mammary epithelial cells failed to form hollow acini when *PER2* and *BMAL1* were knocked down with shRNA.³⁰ Homozygous knockout of *PER1* in mice *in vivo* and decreased abundance in 3D culture had no effects of ductal morphogenesis nor acini formation in culture, supporting the specific role of *PER2* in mammary development. This contrasts with *Clock-Δ19* mice which had poorer milk production related to decreased mammary development during late gestation.¹⁰ It is also important to note that the phenotype that manifests with the deletion of a core clock gene is not necessarily related to the function of the deleted gene, but rather a result of changes in the balance of other circadian clock components.³¹ Thus, when interpreting results, the effect on other circadian clock genes and the loss or decreased ability of cells to coordinate or temporally separate biological processes must be considered. Our previous studies¹¹ and work of others,³² found that the ratio of *BMAL1:CLOCK* to *PER2* abundance increases upon lactogen induced differentiation of HC11 due to increased abundance of *BMAL1* and *CLOCK* and decreased *PER2*. These changes in protein abundance and ratio mirror changes in mammary tissue core clock dynamics between late gestation and the onset of lactation, suggesting a role in the regulation of differentiation of cells for lactation. The relationship of *BMAL1*, *CLOCK* to *PER2* abundance was altered in the sh*CLOCK* and *BMAL1-KO* line in both undifferentiated and lactogen induced differentiated states in 2D cultures.¹⁰

The formation of domes is a morphological indicator of lactogen induced mammary epithelial differentiation in 2D cultures.^{33,34} Previous studies of the sh*CLOCK* line found decreased expression of *CDH1* and *P63* proteins, and in the 2D cultures, sh*CLOCK* cells looked more spindle-shaped rather than the expected cobblestone morphology typical of mammary epithelial cells. Formation of domes under lactogen induced differentiation in 2D cultures is mediated by epithelial-integrin-secreted stroma interactions.³⁵ Cells that undergo epithelial to mesenchyme transition lose epithelial markers and have alterations in integrin-stroma interactions.^{36,37} Decreased expression of *PER2* was also shown to induce epithelial to mesenchyme transition (EMT), and our previous studies found that *PER2* levels were decreased in undifferentiated cultures of the sh*CLOCK* line.^{10,38} Whereas upon lactogen induced differentiation levels of *PER2* increased.

Our studies of *BMAL1-KO* cells in 2D cultures indicate that a lower density across 8-day growth curves was due to cell death rather than decreased proliferation. Cell death was attributed to oxidative stress as *BMAL1-KO* cells had higher levels of reactive oxygen species.⁵ Images captured of undifferentiated *BMAL1-KO* cultures showed the presence of cytoplasmic vacuoles, which is common in processes of cell death.³⁹ However, we found few to no cells dying in 3D cultures across the three lines. This is consistent with the idea that once cells commit to differentiation, cell death pathways are decreased.^{40,41} Thus, cell death cannot account for smaller acini in *BMAL1-KO* and sh*CLOCK* lines.

One possible explanation for the reduced ability to form acini in cells with circadian disruptions is a lack of cellular polarization. Polarization of the epithelial cells of the mammary gland is the final step of development of the mammary gland and is key to the formation of milk-producing acinar structures. In this phase, the epithelial cells elongate and create the typical spherical structures with clear apical and basal membranes, which will separate the lumen from the surrounding ECM.^{42,43} A key feature of polarization is the movement of the nuclei of the acinar cells towards the basal membrane of structure via the actin cytoskeleton.⁴⁴

Our ChIP-seq analysis of BMAL1 transcriptional targets found numerous genes that encoded for proteins that regulate cell-cell adhesion and polarity.⁵ Confocal microscopy during the IF protocol showed that localization of both cell-cell adhesion proteins were found in expected areas; however, their relative abundances in the three cell lines varied significantly. Per unit volume of cell, the shCLOCK line had significantly greater amounts of both cell-cell adhesion proteins compared to the other lines. This contrasts with our analysis of CDH1 abundance in shCLOCK lines in 2D culture systems, which was significantly reduced relative to the wild-type line. The lateral localization of CDH1 in shCLOCK cells in the 3D cultures support that under the combined influence of lactogenic hormones and signals from ECM cells were able to develop basal-apical polarity indicated by localization of the ZO-1 protein and formation of tight junctions typical of epithelial cells. However, we speculate that the greater abundance of CDH1 per unit volume of acini indicates smaller cells and decreased polarization of the shCLOCK cells. In addition, the BMAL1-KO acini had significantly more ZO-1 when compared to the HC11 acini. Thus, surprisingly, the loss of BMAL1 and decreased levels of CLOCK resulted in greater relative abundances of CDH1 and ZO-1 per acini volume. Increased amounts of CDH1 and ZO-1 were associated with the altered shapes of BMAL1-KO and shCLOCK acini. It is possible that the loss of these components of the core molecular clock causes a lack of coordination or communication between tight junction proteins, leading to runaway production of both CDH1 and ZO-1. Further studies are needed to determine if increased CDH1 and ZO-1 relative protein abundances in the BMAL1-KO and shCLOCK acini would inhibit morphogenic changes needed to promote acinar shape and lumen formation.

Transmission electron microscopy of the acini provided insights into the differences of the microstructures of the acini. All three lines exhibited extensive microplicae and convolution of plasma membranes between cells of the acini. Tight junction and adherens junction complexes between cells in HC11 and BMAL1-KO acini appeared normally distributed and well formed; however, shCLOCK acini had decreased evidence of these structures. This is of interest because shCLOCK cells were found to have the greatest amounts of CDH1 and ZO-1 staining per unit volume of cells within acini. Tight junctions and adherens junctions are central to 3D formation of tissues.⁴⁵ Adherens junctions mediate cell-cell adhesion via two transmembrane adhesive receptor sub-complexes: nectins and cadherins. The extracellular domain of nectins and cadherins mediate cell-cell adhesion, while the intracellular regions modulate the assembly of adherens junctions, which create connections to the actin cytoskeleton and cell signaling. CDH1 is the primary cadherin in epithelial cells. Thus, since CDH1 and ZO-1 protein abundance and localization were not reflective of the ability of shCLOCK cells to form tight and adherens junction complexes, other proteins within these complexes may have been altered and warrants further investigations.

HC11 cells in acini showed clear polarization, as indicated by their basally located nuclei. However, the polarization of cells in BMAL1-KO and shCLOCK acini was reduced. This indicates that only the HC11 cells moved through the final process of differentiation to create a structure similar to milk-producing acini with hollow lumens. Possible explanations for these observations include findings that showed the importance of tight junctions and cell-cell adhesions on the polarization of cells within acini.⁴⁶ Without these structures, the various components of the cellular cytoskeleton cannot properly organize to create polarized cells and may explain the reduced ability of BMAL1-KO and shCLOCK cells to polarize.

Spatial-temporal factors are key events in the acquisition of apical-basal polarity. Polarization must be coordinated between all cells in a tissue and results from the integration of polarizing cues from interdependent biological processes that included receptor mediated interactions with the extracellular matrix, cell-cell interactions, and the sensing of diffusible factors.⁴⁷ Circadian clocks generate 24-hour rhythms of cellular functions and are known to time developmental events. These results indicate that clocks in mammary epithelial cells function in the temporal coordination of polarization cues, as disruption of core clock genes decreased polarization and thus interfered with the organization of cells. BMAL1 transcriptional targets identified in HC11 cells were cell adhesion and cell junction mediators, cell polarity (Pard3, Pad3b) genes, and the prolactin receptor.⁵ The BMAL1-KO line had reduced levels of the prolactin receptor in 2D undifferentiated and lactogen differentiated cultures. Prolactin induces apical-basal polarity and maturation of luminal mammary epithelial cells. Prolactin is also an input to the mammary clock.¹¹ Thus,

further studies are needed to elucidate the potential positive-iterative loop of prolactin, circadian clocks, and the timing of tissue developmental events.

In conclusion, loss of BMAL1 or reduction in CLOCK protein limited the size and reduced the ability of mammary epithelial cells to form acini in 3D cultures. The reduced ability of cells to form acini was marked by a reduction in cellular polarity, as evident in TEM images. Polarization is mediated by the coordination of spatial-temporal cues, rather than abundance of cell-cell adhesion proteins. Further studies are now needed to understand the role of clocks in the coordination of events needed for mammary tissue morphogenesis.

Acknowledgements

We would like to thank Dr. Sophie Lelievre and Yunfeng Bai for refining our experimental protocols, Dr. Andy Schaber and the Purdue Imaging Facility for their help with the immunofluorescence image collection and analysis, and Dr. Chris Gilpin and Laurie Mueller for their help with the transmission electron microscopy.

References

1. Saini C, Suter DM, Liani A, Gos P, Schibler U. The mammalian circadian timing system: Synchronization of peripheral clocks. *Cold Spring Harb Symp Quant Biol.* 2011;76:39-47. doi:10.1101/sqb.2011.76.010918
2. Takahashi JS. Transcriptional architecture of the mammalian circadian clock. *Nat Rev Genet.* 2017;18(3):164-179. doi:10.1038/nrg.2016.150
3. Suárez-Trujillo A, Casey TM. Serotonergic and circadian systems: Driving mammary gland development and function. *Front Physiol.* 2016;7(JUL):1-27. doi:10.3389/fphys.2016.00301
4. Minegishi S, Sagami I, Negi S, Kano K, Kitagishi H. Circadian clock disruption by selective removal of endogenous carbon monoxide. *Sci Rep.* 2018;8(1):1-51. doi:10.1038/s41598-018-30425-6
5. Casey T, Suarez-Trujillo A, Cummings S, et al. Core circadian clock transcription factor BMAL1 regulates mammary epithelial cell growth, differentiation, and milk component synthesis. *PLoS One.* 2021;16(8 August). doi:10.1371/journal.pone.0248199
6. Kass L, Erler JT, Dembo M, Weaver VM. Mammary epithelial cell: Influence of extracellular matrix composition and organization during development and tumorigenesis. *Int J Biochem Cell Biol.* 2007;39(11):1987-1994. doi:10.1016/j.biocel.2007.06.025
7. McCaffrey LM, Macara IG. The Par3/aPKC interaction is essential for end bud remodeling and progenitor differentiation during mammary gland morphogenesis. *Genes Dev.* 2009;23(12):1450-1460. doi:10.1101/gad.1795909
8. Casey T, Sun H, Burgess HJ, et al. Delayed Lactogenesis II is Associated With Lower Sleep Efficiency and Greater Variation in Nightly Sleep Duration in the Third Trimester. *J Hum Lact.* 2019;35(4):713-724. doi:10.1177/0890334419830991
9. McCabe CJ, Suarez-Trujillo A, Teeple KA, Casey TM, Boerman JP. Chronic prepartum light-dark phase shifts in cattle disrupt circadian clocks, decrease insulin sensitivity and mammary development, and are

- associated with lower milk yield through 60 days postpartum. *J Dairy Sci.* 2021;104(2):2422-2437. doi:10.3168/jds.2020-19250
10. Casey T, Crodian J, Trujillo AS, et al. CLOCK regulates mammary epithelial cell growth and differentiation. *Am J Physiol - Regul Integr Comp Physiol.* 2016;311(6):R1125-R1134. doi:10.1152/ajpregu.00032.2016
 11. Casey TM, Crodian J, Erickson E, Kuropatwinski KK, Gleiberman AS, Antoch MP. Tissue-Specific Changes in Molecular Clocks During the Transition from Pregnancy to Lactation in Mice¹. *Biol Reprod.* 2014;90(6):1-38. doi:10.1095/biolreprod.113.116137
 12. Burdon TG, Maitland KA, Clark AJ, Wallace R, Watson CJ. Regulation of the sheep β -lactoglobulin gene by lactogenic hormones is mediated by a transcription factor that binds an interferon- γ activation site-related element. *Mol Endocrinol.* 1994;8(11):1528-1536. doi:10.1210/mend.8.11.7877621
 13. Doppler W, Gorner B, Ball RK. Prolactin and glucocorticoid hormones synergistically induce expression of transfected rat β -casein gene promoter constructs in a mammary epithelial cell line. *Proc Natl Acad Sci U S A.* 1989;86(1):104-108. doi:10.1073/pnas.86.1.104
 14. Liu F, Pawliwec A, Feng Z, Yasruel Z, Lebrun JJ, Ali S. Prolactin/Jak2 directs apical/basal polarization and luminal lineage maturation of mammary epithelial cells through regulation of the Erk1/2 pathway. *Stem Cell Res.* 2015;15(2):376-383. doi:10.1016/j.scr.2015.08.001
 15. Bruner HC, Derksen PWB. Loss of E-cadherin-dependent cell–cell adhesion and the development and progression of cancer. *Cold Spring Harb Perspect Biol.* 2018;10(3). doi:10.1101/cshperspect.a029330
 16. Yoh KE, Regunath K, Guzman A, et al. Repression of p63 and induction of EMT by mutant RAS in mammary epithelial cells. *Proc Natl Acad Sci U S A.* 2016;113(41):E6107-E6116. doi:10.1073/pnas.1613417113
 17. Yang N, Williams J, Pekovic-Vaughan V, et al. Cellular mechano-environment regulates the mammary circadian clock. *Nat Commun.* 2017;8:1-28. doi:10.1038/ncomms14287
 18. Lo AT, Mori H, Mott J, Bissell MJ. Constructing three-dimensional models to study mammary gland branching morphogenesis and functional differentiation. *J Mammary Gland Biol Neoplasia.* 2012;17(2):103-110. doi:10.1007/s10911-012-9251-7
 19. Vidi PA, Bissell MJ, Lelièvre SA. Three-dimensional culture of human breast epithelial cells: The how and the why. *Methods Mol Biol.* 2013;945:193-219. doi:10.1007/978-1-62703-125-7_13
 20. Shamir ER, Ewald AJ. Three-dimensional organotypic culture: Experimental models of mammalian biology and disease. *Nat Rev Mol Cell Biol.* 2014;15(10):647-664. doi:10.1038/nrm3873
 21. Pal A, Kleer CG. Three dimensional cultures: A tool to study normal acinar architecture vs. malignant transformation of breast cells. *J Vis Exp.* 2014;(86). doi:10.3791/51311
 22. Martin F, Stein T, Howlin J. *Mammary Gland Development: Methods and Protocols.* Vol 1501.; 2017.

23. Okada M, Hersh D, Paul E, Van Der Straaten D. Effect of centration and circularity of manual capsulorrhexis on cataract surgery refractive outcomes. *Ophthalmology*. 2014;121(3):763-770. doi:10.1016/j.ophtha.2013.09.049
24. Zhang JQ, Li YM, Liu T, et al. Antitumor effect of matrine in human hepatoma G2 cells by inducing apoptosis and autophagy. *World J Gastroenterol*. 2010;16(34):4281-4290. doi:10.3748/wjg.v16.i34.4281
25. Pitelka DR, Hamamoto ST. Form and function in Mammary Epithelium: The Interpretation of Ultrastructure. *J Dairy Sci*. 1977;60(4):643-654. doi:10.3168/jds.S0022-0302(77)83914-3
26. Chaix A, Zarrinpar A, Panda S. The circadian coordination of cell biology. *J Cell Biol*. 2016;215(1):15-25. doi:10.1083/jcb.201603076
27. Looby P, Loudon A. Gene duplication and complex circadian clocks in mammals. *Trends Genet*. doi:10.1016/j.tig.2004.11.012
28. Gibson TJ, Spring J. Genetic redundancy in vertebrates: Polyploidy and persistence of genes encoding multidomain proteins. *Trends Genet*. 1998;14(2):46-49. doi:10.1016/S0168-9525(97)01367-X
29. McQueen CM, Schmitt EE, Sarkar TR, et al. PER2 regulation of mammary gland development. *Dev*. 2018;145(6):1-10. doi:10.1242/dev.157966
30. Rossetti S, Corlazzoli F, Gregorski A, Azmi NHA, Sacchi N. Identification of an estrogen-regulated circadian mechanism necessary for breast acinar morphogenesis. *Cell Cycle*. 2012;11(19):3691-3700. doi:10.4161/cc.21946
31. Nelson WJ. Remodeling epithelial cell organization: transitions between front-rear and apical-basal polarity. *Cold Spring Harb Perspect Biol*. 2009;1(1):1-19. doi:10.1101/cshperspect.a000513
32. Metz RP, Qu X, Laffin B, Earnest D, Porter WW. Circadian clock and cell cycle gene expression in mouse mammary epithelial cells and in the developing mouse mammary gland. *Dev Dyn*. 2006;235(1):263-271. doi:10.1002/dvdy.20605
33. Morrison B, Cutler M Lou. Mouse mammary epithelial cells form mammospheres during lactogenic differentiation. *J Vis Exp*. 2009;(32):1-2. doi:10.3791/1265
34. Desrivières S, Prinz T, Castro-Palomino Laria N, et al. Comparative proteomic analysis of proliferating and functionally differentiated mammary epithelial cells. *Mol Cell Proteomics*. 2003;2(10):1039-1054. doi:10.1074/mcp.M300032-MCP200
35. Wang W, Morrison B, Galbaugh T, Jose CC, Kenney N, Cutler M Lou. Glucocorticoid induced expression of connective tissue growth factor contributes to lactogenic differentiation of mouse mammary epithelial cells. *J Cell Physiol*. 2008;214(1):38-46. doi:10.1002/jcp.21159
36. Zhu C, Kong Z, Wang B, Cheng W, Wu A, Meng X. ITGB3/CD61: A hub modulator and target in the tumor microenvironment. *Am J Transl Res*. 2019;11(12):7195-7208.

37. Bhowmick NA, Zent R, Ghiassi M, McDonnell M, Moses HL. Integrin β 1 Signaling is Necessary for Transforming Growth Factor- β Activation of p38MAPK and Epithelial Plasticity. *J Biol Chem.* 2001;276(50):46707-46713. doi:10.1074/jbc.M106176200
38. Hwang-Verslues WW, Chang PH, Jeng YM, et al. Loss of corepressor PER2 under hypoxia up-regulates OCT1-mediated EMT gene expression and enhances tumor malignancy. *Proc Natl Acad Sci U S A.* 2013;110(30):12331-12336. doi:10.1073/pnas.1222684110
39. Shubin A V., Demidyuk I V., Komissarov AA, Rafieva LM, Kostrov S V. Cytoplasmic vacuolization in cell death and survival. *Oncotarget.* 2016;7(34):55863-55889. doi:10.18632/oncotarget.10150
40. Lu QL, Abel P, Foster CS, Lalani EN. bcl-2: Role in epithelial differentiation and oncogenesis. *Hum Pathol.* 1996;27(2):102-110. doi:10.1016/S0046-8177(96)90362-7
41. Wagner KU, Boulanger CA, Henry MLD, Sgagias M, Hennighausen L, Smith GH. An adjunct mammary epithelial cell population in parous females: Its role in functional adaptation and tissue renewal. *Development.* 2002;129(6):1377-1386. doi:10.1242/dev.129.6.1377
42. Oakes SR, Hilton HN, Ormandy CJ. Key stages in mammary gland development: The alveolar switch: Coordinating the proliferative cues and cell fate decisions that drive the formation of lobuloalveoli from ductal epithelium. *Breast Cancer Res.* 2006;8(2):1-21. doi:10.1186/bcr1411
43. Chin AR, Yan W, Cao M, Liu X, Wang SE. Polarized Secretion of Extracellular Vesicles by Mammary Epithelia. *J Mammary Gland Biol Neoplasia.* 2018;23(3):165-176. doi:10.1007/s10911-018-9402-6
44. Gundersen GG, Worman HJ. Nuclear positioning. *Cell.* 2013;152(6):1376-1389. doi:10.1016/j.cell.2013.02.031
45. Campbell HK, Maiers JL, DeMali KA. Interplay between tight junctions & adherens junctions. *Exp Cell Res.* 2017;358(1):39-44. doi:10.1016/j.yexcr.2017.03.061
46. Lelièvre SA. Tissue polarity-dependent control of mammary epithelial homeostasis and cancer development: An epigenetic perspective. *J Mammary Gland Biol Neoplasia.* 2010;15(1):49-63. doi:10.1007/s10911-010-9168-y
47. Bryant DM, Mostov KE. From cells to organs: Building polarized tissue. *Nat Rev Mol Cell Biol.* 2008;9(11):887-901. doi:10.1038/nrm2523